

High-performance 1–3-type composites based on $(1 - x)\text{Pb}(A_{1/3}\text{Nb}_{2/3})\text{O}_3 - x\text{PbTiO}_3$ single crystals ($A = \text{Mg}, \text{Zn}$)

S V Bezus¹, V Yu Topolov¹ and C R Bowen²

¹ Department of Physics, Rostov State University, 5 Zorge Street, 344090 Rostov-on-Don, Russia

² Materials Research Centre, Department of Mechanical Engineering, University of Bath, BA2 7AY Bath, UK

E-mail: topolov@phys.rsu.ru

Received 30 September 2005, in final form 21 February 2006

Published 20 April 2006

Online at stacks.iop.org/JPhysD/39/1919

Abstract

This paper describes the concentration dependences of piezoelectric coefficients, squared figures of merit and electromechanical coupling factors which have been calculated for 1–3 and 1–0–3 piezo-active composites based on single crystals of relaxor-ferroelectric solid solutions of $(1 - x)\text{Pb}(A_{1/3}\text{Nb}_{2/3})\text{O}_3 - x\text{PbTiO}_3$ where $A = \text{Mg}, \text{Zn}$. The role of the single-crystal component, its electromechanical properties and the polymer matrix (monolithic or porous) in forming these concentration dependences is analysed to demonstrate the ranges in which effective composite parameters are most sensitive to material properties and composite architecture, with particular emphasis on where their maximum values are attained. The basic variables in this study are the chemical composition (x and A), volume concentrations of the single-crystal component, the presence of pores in the polymer matrix and the aspect ratio of the spheroidal pores. It has been shown that particularly high values of piezoelectric coefficient $g_{33}^* \sim 10^2 \text{ mV m N}^{-1}$ and hydrostatic piezoelectric coefficients $g_h^* \sim 10^2 \text{ mV m N}^{-1}$ and $d_h^* \sim (10^2 - 10^3) \text{ pC N}^{-1}$ are expected in the 1–0–3 $0.67\text{Pb}(\text{Mg}_{1/3}\text{Nb}_{2/3})\text{O}_3 - 0.33\text{PbTiO}_3$ single crystal / porous araldite composite with spheroidal pores in the matrix.

1. Introduction

Due to their excellent electromechanical properties near the morphotropic phase boundary [1, 2], single crystals of relaxor-ferroelectric solid solutions of $(1 - x)\text{Pb}(\text{Mg}_{1/3}\text{Nb}_{2/3})\text{O}_3 - x\text{PbTiO}_3$ (PMN- x PT) and $(1 - x)\text{Pb}(\text{Zn}_{1/3}\text{Nb}_{2/3})\text{O}_3 - x\text{PbTiO}_3$ (PZN- x PT) are of interest for many piezotechnical applications, e.g. as active elements of sensors, actuators or piezoelectric transducers and as a component of modern piezo-active composites [3–5]. These single crystals, whose compositions are in the vicinity of the morphotropic phase boundary at room temperature, are characterized by a variety of domain and heterophase structures [1, 6], domain switching and rotation effects, high piezoelectric activity and considerable dielectric permittivities, elastic compliances and

electromechanical coupling factors [2–4, 7–11]. Recently, full sets of the piezoelectric, dielectric and elastic constants have been experimentally determined for a variety of compositions of the above-mentioned single crystals. For example, these property sets are known for (001) cuts (related to the perovskite unit-cell axes) for multidomain PMN- x PT single crystals with $x = 0.30, 0.33$ and 0.42 (4 mm symmetry) [2, 10, 11] and multidomain PZN- x PT single crystals with $x = 0.045, 0.07$ and 0.08 (4 mm symmetry) [3, 7, 8] as well as for single-domain PMN-0.33PT crystal samples with 3 m symmetry. All the above-mentioned electromechanical constants have been measured at room temperature.

The application of the above-mentioned single crystals as piezo-active components of advanced composites has been discussed in a series of recent papers. Experimental papers [3–5]

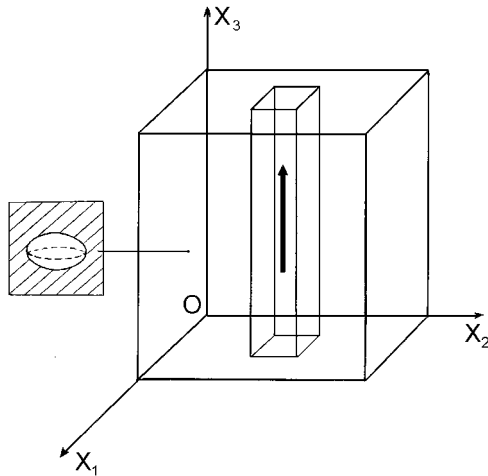


Figure 1. Schematic diagram of the 1–3-type composite. The spontaneous polarization vector of the single crystal is denoted by an arrow. $X_1X_2X_3$ is the rectangular coordinate system. A spheroidal air pore is shown in the inset.

related to this subject are concerned with performances of single crystal/polymer composites, such as 0–3 composites based on PMN–0.35PT and 1–3 composites based on PZN–0.08PT or PMN–0.33PT. The active role of the relaxor-ferroelectric single-crystal components in forming the piezoelectric properties of 0–3 and 0–1–3 composites was analysed in a recent work [12]. With regard to composites with 1–3 connectivity, it is of interest to undertake a comparative study of a variety of possible single crystal/polymer composites. The effect of electromechanical properties of the PMN– x PT or PZN– x PT single crystals on composite properties is to be studied, along with a thorough examination of the use of a porous polymer matrix to further improve composites performance. The main aim of the present paper is the determination and analysis of important concentration dependences of the effective parameters of the 1–3-type composites based on PMN– x PT or PZN– x PT single crystals with compositions chosen near the morphotropic phase boundary.

2. Structure of 1–3-type composites and features of their effective parameters

2.1. Structure and effective electromechanical properties of 1–3 and 1–0–3 composites

Consider a composite sample (figure 1) poled by an electric field $\mathbf{E} \parallel OX_3$ and containing a system of single-crystal rods in the form of rectangular parallelepipeds which are continuous in the OX_3 direction. Lateral crystal faces are parallel to the (X_1OX_3) and (X_2OX_3) planes related to the coordinate system $X_1X_2X_3$. The main crystallographic axes x , y and z of each single crystal with 4mm symmetry are oriented as follows: $x \parallel OX_1$, $y \parallel OX_2$ and $z \parallel OX_3$. It is assumed that the rods are regularly distributed in a polymer matrix which can be monolithic or porous. In the last case, the matrix contains a system of regularly distributed spherical or spheroidal air inclusions that occupy the sites of a simple cubic or tetragonal lattice, respectively. The radius or the largest semi-axis of these pores should be considerably less than the length of

the side of the square being the intersection of the rod by the (X_1OX_2) plane. The above-described composite sample with the monolithic or porous matrix is described by the 1–3 or 1–0–3 connectivity, respectively. As is the case for the manufactured 1–3 composites [3], it is assumed that the poling procedure is carried out after inserting the aligned rods into the matrix and covering the composite sample with electrodes parallel to the (X_1OX_2) plane.

The determination of the effective electromechanical properties of the system ‘rods with the volume concentration m —matrix with the volume concentration $1 - m$ ’ is carried out using the matrix method [13, 14]. The volume concentration m is defined as the ratio of the total volume of the rods to the volume of the composite sample. The matrix method is based on averaging the electromechanical constants of the rods and the matrix in the OX_1 and OX_2 directions [14], in which the regular (periodical) structure of the composite is observed. The electromechanical constants (i.e. full sets of elastic compliances s_{ij}^E measured at constant electric field E , piezoelectric coefficients d_{kl} and dielectric permittivities $\varepsilon_{ff}^{\sigma}$ measured at constant stress σ) of both the components of any symmetry are averaged by taking into account boundary conditions [13] for the electric and mechanical fields. These boundary conditions at $x_i = \text{constant}$ correspond to the continuity of three normal components of the mechanical stress σ_{iv} , three tangential components of the mechanical strain ξ_{rt} , one normal component of the electric displacement D_i and two tangential components of the electric field E_j where $i = 1$ or 2 , $v = 1, 2, 3$. The subscripts r, t and j are not equal to i and can ‘have’ values 1, 2 or 3.

In the case of the 1–0–3 composite, we first calculate the effective constants of the polymer matrix with aligned spheroidal pores (that occupy the sites of a simple cubic lattice) and its dependence on m_p , where m_p is the ratio of the total volume of the pores to the volume of the matrix. The corresponding averaging procedure is carried out by means of the effective field method [15] based on Eshelby’s concept of spheroidal inclusions [16, 17]. As follows from our consideration, the porous matrix is characterized as a transversely isotropic medium. Our further calculations are carried out using the experimental room-temperature electromechanical constants of the PMN– x PT [2, 10] and PZN– x PT [3, 4, 7, 8] single crystals and polymers [18–20].³ As a result, we obtain concentration dependences of the full set of the effective elastic compliances $s_{ij}^{*E}(m, m_p)$, piezoelectric coefficients $d_{kl}^{*}(m, m_p)$ and dielectric permittivities $\varepsilon_{ff}^{*\sigma}(m, m_p)$ of the studied 1–0–3 or 1–3 (for $m_p = 0$) composites. Based on these effective parameters and formulae [18–21], one can evaluate the piezoelectric coefficients $\|e^*\| = \|d^*\| \cdot \|s^{*E}\|^{-1}$, $\|g^*\| = \|d^*\| \cdot \|\varepsilon^{*\sigma}\|^{-1}$ and $\|h^*\| = \|e^*\| \cdot \|\varepsilon^{*\xi}\|^{-1}$, squared figure of merit $(Q_{33}^*)^2 = d_{33}^*g_{33}^*$, hydrostatic parameters $d_h^* = d_{33}^* + d_{32}^* + d_{31}^*$, $g_h^* = d_h^*/\varepsilon_{33}^{*\sigma}$, $(Q_h^*)^2 = d_h^*g_h^*$, electromechanical coupling factors $k_{33}^* = d_{33}^*(s_{33}^{*E}\varepsilon_{33}^{*\sigma})^{-1/2}$, $k_t^* = e_{33}^*(c_{33}^{*D}\varepsilon_{33}^{*\xi})^{-1/2}$, etc where $\|\varepsilon^{*\xi}\|$ is the matrix of dielectric permittivities measured at constant strain ξ , c_{33}^{*D} is the elastic modulus measured at constant electric displacement D . The matrix of the elastic

³ Hereafter we denote the electromechanical constants of the single-crystal rod and the surrounding matrix by subscripts ‘ c ’ and ‘ m ’, respectively. The effective constants of the composite are denoted by an asterisk.

Table 1. Maximum values of effective parameters g_{33}^* (in mV m N⁻¹), h_{33}^* (in 10⁸ V m⁻¹), d_h^* (in pC N⁻¹), g_h^* (in mV m N⁻¹), k_t^* , $(Q_{33}^*)^2$ (in 10⁻¹² Pa⁻¹), and $(Q_h^*)^2$ (in 10⁻¹² Pa⁻¹) which have been calculated for the 1–3 relaxor-ferroelectric single crystal/araldite composites.

Single-crystal component	max g_{33}^*	max h_{33}^*	max d_h^*	max g_h^*	max k_t^*	max $((Q_{33}^*)^2)$	max $((Q_h^*)^2)$
PMN–0.30PT	382 (0.013) ^a	26.1 (0.414-0.547)	244 (0.434)	103 (0.013)	0.819 (0.552)	106 (0.160)	6.16 (0.099)
PMN–0.33PT	496 (0.017)	37.8 (0.501-0.532)	274 (0.509)	130 (0.016)	0.861 (0.559)	144 (0.250)	7.45 (0.115)
PMN–0.42PT	519 (0.024)	56.9 (0.653-0.709)	— ^b	140 (0.024)	0.729 (0.640)	46.3 (0.078)	3.46 (0.082)
PZN–0.045PT	317 (0.021)	19.5 (0.311-0.389)	180 (0.438)	81.0 (0.019)	0.720 (0.532)	108 (0.338)	4.62 (0.141)
PZN–0.07PT	359 (0.023)	23.1 (0.419-0.480)	194 (0.455)	93.9 (0.021)	0.750 (0.537)	133 (0.460)	5.43 (0.146)
PZN–0.08PT	352 (0.019)	22.3 (0.334-0.390)	206 (0.409)	90.6 (0.018)	0.765 (0.422)	136 (0.422)	5.38 (0.131)

^a The optimal volume concentrations m_{opt} of the single-crystal component which correspond to the maximum values (i.e. $\max Y^* = Y^*(m_{\text{opt}}, 0)$ in our notations given in sections 2.1 and 2.2) are written in parentheses. In the h_{33}^* column, ranges of the volume concentrations obey a condition $\max h_{33}^* - h_{33}^*(m, 0) \leq 10^7 \text{ V m}^{-1}$.

^b For this composite, the monotonous concentration dependence $d_h^*(m, 0)$ has been established.

moduli $\|c^{*D}\|$ is determined using, for example, the relation [21] $\|h^*\| = \|g^*\| \cdot \|c^{*D}\|$.

2.2. Maxima of effective parameters of 1–3-type composites

Table 1 and figures 2 and 3 show some results related to the maxima of different effective parameters of the 1–3 composites. Among the six single-crystal components, of particular interest are PMN–0.42PT and PMN–0.33PT. The use of PMN–0.42PT single crystal as the active material enables the composite to attain large maximum values of parameters as follows: $\max g_{33}^*(m, 0) = 19.3g_{33,c}$, $\max g_h^*(m, 0) = 23.3g_{h,c}$ and $\max h_{33}^*(m, 0) = 1.08h_{33,c}$. The above-mentioned and other parameters of the PMN– x PT and PZN– x PT single crystals being used as the piezo-active components of the studied composites are listed in table 2 for a further comparison. The piezoelectric response of the corresponding 1–3 composite is closely associated with the relatively low dielectric permittivity of the PMN–0.42PT single crystal: the measured value $\varepsilon_{33,c}^\sigma/\varepsilon_0 = 660$ is one order of magnitude smaller than $\varepsilon_{33,c}^\sigma/\varepsilon_0$ of the other single-crystal PMN– x PT samples (see table 2) with compositions across the morphotropic phase boundary ($0.30 \leq x \leq 0.33$) [10]. Despite the low volume concentrations $0.01 < m_{\text{opt}} < 0.02$ corresponding to $\max g_{33}^*(m, 0)$ and $\max g_h^*(m, 0)$ (see table 1 and curves 1 in figures 2(a) and (b)) as well as an inequality $\varepsilon_{33}^{*\sigma}(m_{\text{opt}}, 0) \ll \varepsilon_{33,c}^\sigma$, the PMN– x PT-based composites with $x = 0.33$ or 0.42 are of interest at $0.05 < m < 0.1$: in this concentration range $g_{33}^*(m, 0)/g_{33,c} \approx 8$ –13 and $g_h^*(m, 0)/g_{h,c} \approx 10$ –15. In contrast to $g_{33}^*(m, 0)$, the practical constancy of $h_{33}^*(m, 0)$ for $0.1 < m < 0.9$ (curve 1 in figure 2(c)) is associated with the boundary conditions for the electric field and mechanical strain components at $x_j = \text{const}$ ($j = 1; 2$) and, as a consequence, with an equation $e_{33}^*(m, 0)/e_{33,c} \approx \varepsilon_{33}^{*\xi}(m, 0)/\varepsilon_{33,c}^\xi$ that holds true for all the 1–3 composites studied in this work.

It should be added that using the porous polymer matrix (e.g. with spherical pores at $0 < m_p \leq 0.3$) rather than a monolithic polymer matrix results in only a modest change in $h_{33}^*(m, m_p)$ (compare curves 1 and 2 in figure 2(c)) because interrelations $e_{33}^*(m, m_p)/e_{33,c} \approx \varepsilon_{33}^{*\xi}(m, m_p)/\varepsilon_{33,c}^\xi$ and $\varepsilon_{33}^{*\xi}(m, m_p) \ll \varepsilon_{33,c}^\xi$ are correct in the wide m range.

The PZN–0.08PT-based 1–3 composite is characterized by the large $\max[Q_{33}^*(m, 0)]^2$ value (see table 1) which is mainly explained by considerable values of the piezoelectric

coefficient $d_{33,c}$ and the dielectric permittivity $\varepsilon_{33,c}^\sigma$ of the single-crystal component (see table 2). In addition, the corresponding m_{opt} value is nearly equal to that determined for $\max d_h^*(m, 0)$, and such closeness is not typical of the other 1–3 composite systems shown in table 1. However, the 1–3 composite based on PZN–0.08PT does not possess large values of $\max g_{33}^*(m, 0)$, $\max d_h^*(m, 0)$ and $\max g_h^*(m, 0)$, and as a consequence, a ratio $\max[Q_{33}^*(m, 0)]^2/\max[Q_h^*(m, 0)]^2 \approx 25$ becomes the highest value for the composites from table 1. Such features are associated with the elastic and piezoelectric properties of the single-crystal component forming the piezoelectric response of the 1–3 composite. In addition, the elastic and piezoelectric anisotropy of the rods as well as differences between the elastic constants of the rod and the matrix considerably influence the piezoelectric sensitivity and the hydrostatic parameters of the 1–3 composite, as shown [22] for the ferroelectric ceramic-based composites. It should be noted that the maximum values of the effective parameters calculated for the PZN– x PT-based composites are located in fairly narrow ranges for each composition (see table 1). This behaviour is accounted for by monotonous dependences $s_{ij,c}^E(x)$, $d_{3f,c}(x)$ and $\varepsilon_{ff,c}^\sigma(x)$ of the PZN– x PT single crystals [3, 7, 8] where $ij = 11, 12, 13$ and $f = 1, 3$. This is true despite considerable changes in the values of some electromechanical constants. For example, the changes in $d_{3f,c}(x)$ and $\varepsilon_{33,c}^\sigma(x)$ attain 50% in the molar concentration range $0.045 \leq x \leq 0.08$, and the dependence $s_{12,c}^E(x)$ provides a ratio $s_{12,c}^E(0.045)/s_{12,c}^E(0.08) \approx 2.2$.

The high values of $\max d_h^*(m, 0) = 1.71d_{h,c}$, $\max k_t^*(m, 0) = 1.25k_{t,c}$, $\max[Q_{33}^*(m, 0)]^2 = 1.31(Q_{33,c})^2$ and $\max[Q_h^*(m, 0)]^2 = 21.1(Q_{h,c})^2$ are attained in the PMN–0.33PT-based 1–3 composite due to the composition lying close to the morphotropic phase boundary [1]. As a consequence, the PMN–0.33PT single crystal is characterized [2, 10] by the largest values of the elastic compliances $|s_{33,c}^E|$, piezoelectric coefficients $|d_{3j,c}|$ and dielectric permittivity $\varepsilon_{33,c}^\sigma$ in the range $0.30 \leq x \leq 0.42$. These prominent performances strongly influence the effective electromechanical properties of the related composite. A further comparison of the calculated and known experimental parameters of the PMN–0.33PT-based 1–3 composite is shown in table 3. It is seen that the good agreement between the calculated and experimental values is attained at various volume concentrations of the single-crystal rods. Some differences between these values can be associated with the finite sizes of the rods and their piezoelectric and

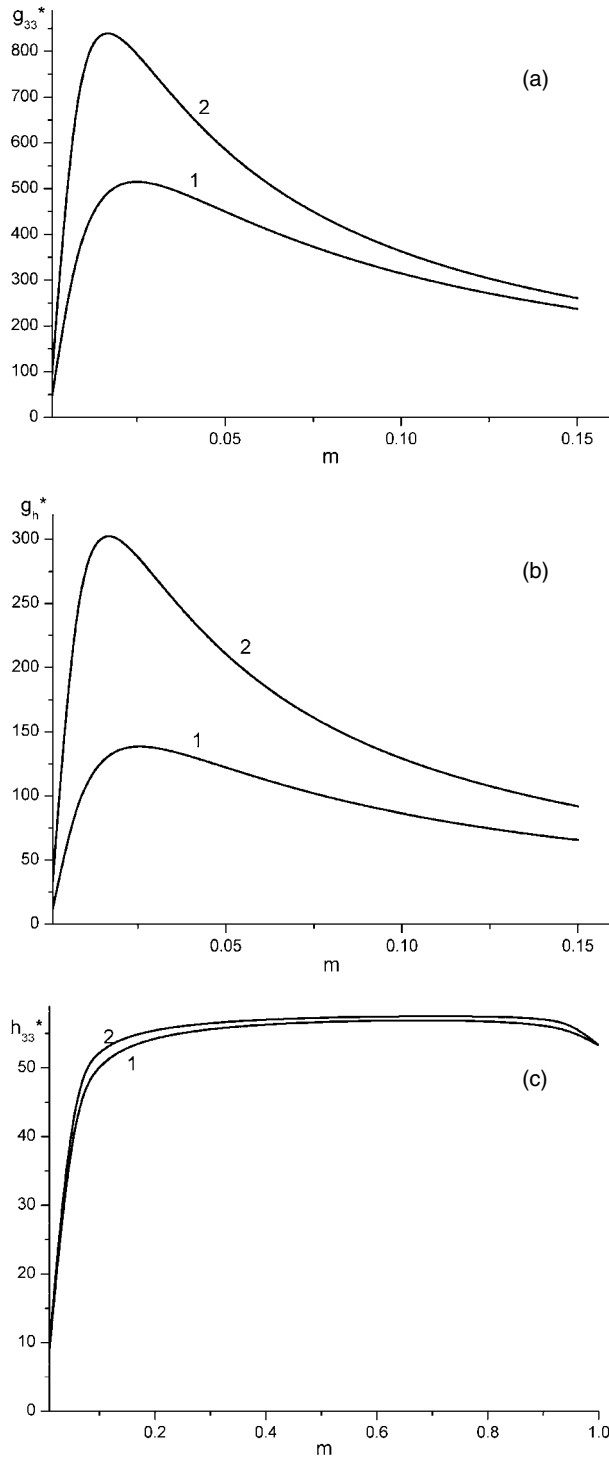


Figure 2. Concentration dependences of the piezoelectric coefficients: (a) g_{33}^* in mV N^{-1} , (b) g_h^* in mV N^{-1} and (c) h_{33}^* in 10^8 V m , which have been calculated for the PMN-0.42PT single crystal/araldite (curve 1) and PMN-0.42PT single crystal/porous araldite ($m_p = 0.3$) (curve 2) composites. The porous matrix contains spherical pores.

dielectric properties. For example, the experimental $d_{33,c}$ and $\varepsilon_{33,c}^\sigma$ values from [4] are less than those from the complete set of the electromechanical constants measured in the work [2].

In addition to the active piezoelectric component, the use of a porous matrix with the regularly-distributed

spherical pores leads to an increase in a series of the effective parameters of the 1–0–3 composites, as compared with the related 1–3 composites (see, e.g. curves 1 and 2 in figures 2 and 3). The 1–0–3 PMN-0.33PT / porous araldite ($m_p = 0.3$) composite is of practical interest because of high values of $\max k_t^*(m, 0.3) = 1.32k_{t,c}$, $\max d_h^*(m, 0.3) = 2.66d_{h,c}$, $\max [Q_{33}^*(m, 0.3)]^2 = 2.19(Q_{33,c})^2$, and $\max [Q_h^*(m, 0.3)]^2 = 72.6(Q_{h,c})^2$. These and other related parameters open up new possibilities of creating advanced piezo-active composites containing the relaxor-ferroelectric components. The maximum values of the above-mentioned parameters are higher than those measured on 1–3 composites containing ceramic or single-crystal rods. For example, the experimental values of $\max k_t^*$ are 0.83, 0.80 and 0.70 for the PZN-0.08PT single crystal / polymer [3], PMN-0.33PT single crystal/epoxy [4] and PZT-7A ceramic/polymer [18] composites, respectively. The experimental $\max d_h^*$ value known for the PZT-7A ceramic/Spurr epoxy composite [18] does not exceed 120 pC N^{-1} .

An increase in the porosity m_p in the polymer matrix of the 1–0–3 composite promotes an increase in $g_{33}^*(m, m_p)$, $g_h^*(m, m_p)$, $d_h^*(m, m_p)$, $[Q_{33}^*(m, m_p)]^2$ and $[Q_h^*(m, m_p)]^2$ in a wide m range as compared with the case of $m_p = 0$ (see curves 1 and 2 in figures 2(a), (b) and 3(a), (c) and (d)). Increasing $d_h^*(m, m_p)$ in comparison with $d_h^*(m, 0)$ (see figure 3(a) and table 4) correlates with changes in the $c_{11,m}/c_{12,m}$ ratio of the elastic moduli of the porous matrix. The piezoelectric coefficient $d_{33}^*(m, m_p)$, that describes the piezoelectric activity of the 1–0–3 composite along the axis OX_3 , increases faster than $|d_{31}^*(m, m_p)|$ with respect to the volume concentration m . It stems from the fact that piezoelectric interaction between the rods in the (X_1OX_2) plane is reduced to a greater degree by a porous matrix than by a monolithic matrix. This circumstance favours an increase in $\max d_h^*(m, m_p)$ at $m_p = \text{const}$ as follows from table 4. A change in the balance between $d_{33}^*(m, m_p)$ and $d_{31}^*(m, m_p)$ is caused by changes in $c_{11,m}/c_{12,m}$ and elastic stiffness of the matrix. In particular, as seen from table 4, increasing $c_{11,m}$ results in highest volume concentrations m_{opt} related to $\max d_h^*$, this shift takes place for both the 1–3 and 1–0–3 composites. In the 1–0–3 composites studied, the higher m_{opt} value corresponds to the lower $c_{11,m}/c_{12,m}$ ratio. Such correlation between $\max d_h^*$ and $c_{11,m}/c_{12,m}$ enables us to predict the hydrostatic piezoelectric activity of the 1–0–3 composites based on the relaxor-ferroelectric single crystals.

2.3. Spheroidal pores in the matrix and piezoelectric response of 1–0–3 composites

Another interesting aspect of the problem of the porous matrix is concerned with its microgeometry. We assume that the matrix contains aligned oblate spheroidal pores being regularly distributed (see inset in figure 1⁴). The shape of these

⁴ According to the data from the ISIS Innovation (Technology Transfer from the University of Oxford, UK, project Nr 704), academics at the University of Oxford have produced a permeable material containing pores of exactly the same size and shape, separated by a regular spacing [23]. The invention is based on the physical regularity of an interference pattern. In this case a polymer is exposed to an interference pattern giving rise to a predetermined matrix of cross-linked material. This provides the blueprint for an exceptionally regular array of pores. This process is highly controllable, continuously variable and allows us to control the variation in the pore size, shape and periodicity.

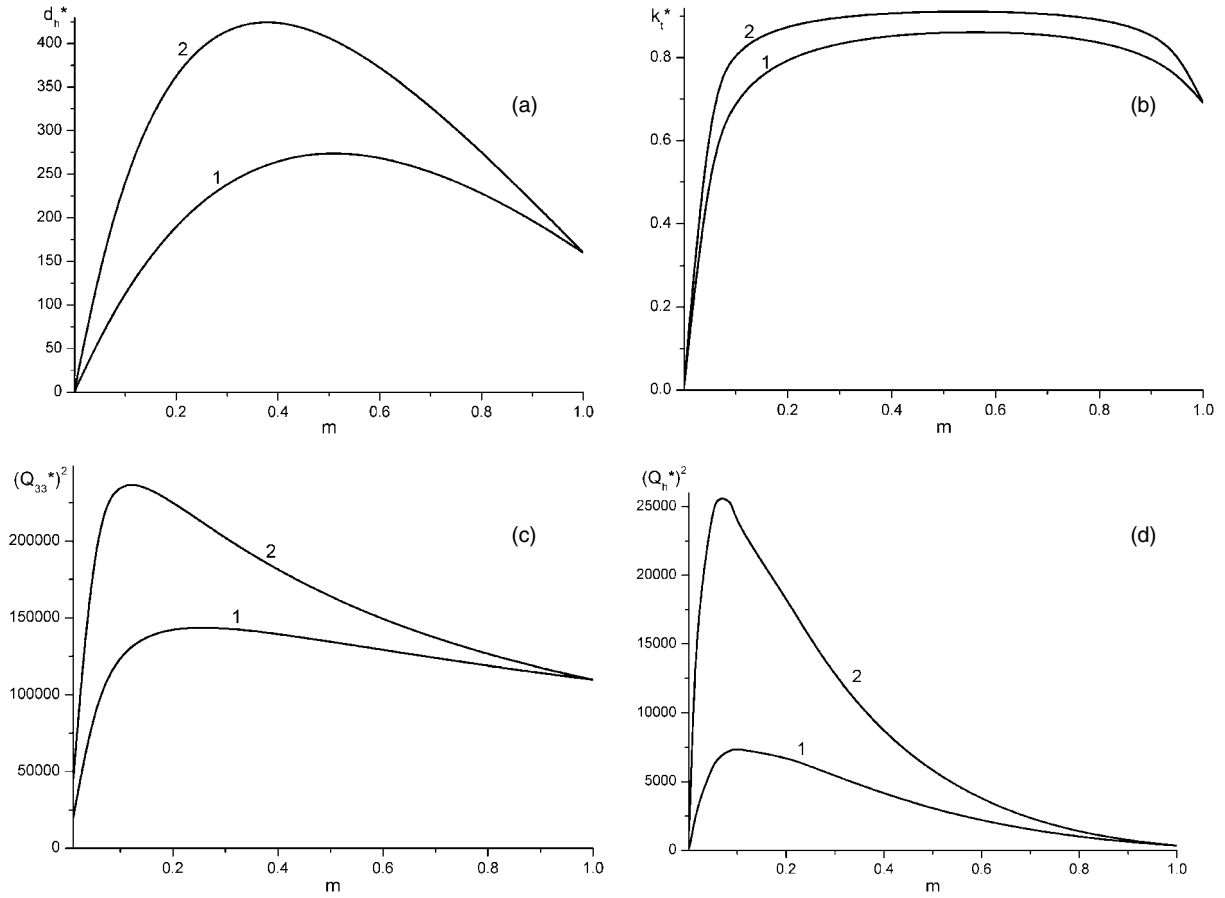


Figure 3. Concentration dependences of (a) the hydrostatic piezoelectric coefficient d_h^* in pC N^{-1} , (b) electromechanical coupling factor k_t^* , (c) the squared figure of merit $(Q_{33}^*)^2$ in 10^{-15} Pa^{-1} , and (d) the squared hydrostatic figure of merit $(Q_h^*)^2$ in 10^{-15} Pa^{-1} , which have been calculated for the PMN–0.33PT single crystal / araldite (curve 1) and PMN–0.33PT single crystal/porous araldite ($m_p = 0.3$, spherical pores) (curve 2) composites.

Table 2. Experimental values of the room-temperature electromechanical constants of the relaxor-ferroelectric single crystals.

Single crystal	$d_{33,c}$ (pC N^{-1})	$g_{33,c}$ (mV m N^{-1})	$h_{33,c}$ (10^8 V m^{-1})	$d_{h,c}$ (pC N^{-1})	$g_{h,c}$ (mV m N^{-1})	$\varepsilon_{33,c}^s/\varepsilon_0$	$k_{t,c}$	$(Q_{33,c})^2$ (10^{-12} Pa^{-1})	$(Q_{h,c})^2$ (10^{-12} Pa^{-1})
PMN–0.30PT [10]	1981	28.7	24.6	139	2.1	7800	0.62	56.9	0.292
PMN–0.33PT [2]	2820	38.8	33.7	160	2.0	8200	0.64	109	0.320
PMN–0.42PT [10]	260	44.5	53.2	78	13.4	660	0.62	11.6	1.05
PZN–0.045PT [7]	2000	44.0	17.0	60	2.0	5200	0.50	88.0	2.64
PZN–0.07PT [8]	2455	49.3	20.7	47	0.9	5622	0.47	121	0.423
PZN–0.08PT [3]	2890	42.4	17.7	–20	–0.2	7700	0.45	123	0.004

Table 3. Calculated and experimental (in parentheses, [4]) values of normalized parameters^a of the 1–3 PMN–0.33PT single crystal/epoxy composite.

m	0.37	0.48	0.62	0.77
$k_t^*/k_{t,c}$	1.32 (1.30)	1.34 (1.36)	1.35 (1.38)	1.31 (1.34)
$c_{33}^{*D}/c_{33,c}^D$	0.295 (0.300)	0.371 (0.332)	0.474 (0.431)	0.605 (0.598)

^a The $k_t^*/k_{t,c}$ and $c_{33}^{*D}/c_{33,c}^D$ ratios have been calculated using the room-temperature electromechanical constants of the PMN–0.33PT single crystal [2] and epoxy [4].

inclusions is described by an equation $(x_1/a_1)^2 + (x_2/a_1)^2 + (x_3/a_3)^2 = 1$ in the coordinate system $X_1X_2X_3$, where a_j are the semi-axes of the spheroid. The volume concentration of the single-crystal rods m , the porosity m_p and the aspect ratio $\rho = a_1/a_3$ become three independent arguments that influence the effective parameters $Y^* = Y^*(m, m_p, \rho)$ of the studied

1–0–3 composites. In this section we analyse the features of the piezoelectric response of the 1–0–3 composites based on PMN–0.33PT at $m_p = 0.3$.

First, even at relatively small aspect ratios ($2 \leq \rho \leq 5$) $\max g_{33}^*(m, 0.3, \rho)$ and $\max g_h^*(m, 0.3, \rho)$ are attained at $0.005 < m < 0.01$, and such microgeometry of the

Table 4. Values of $\max d_h^*$ (in pC N^{-1}), m_{opt}^a (at $m_p = \text{const}$)^b and $c_{11,m}/c_{12,m}$ which have been calculated for the 1–3-type composites based on PMN–0.33PT single crystals.

Components	$\max d_h^*$	m_{opt}	$c_{11,m}/c_{12,m}$
Polyethylene ($m_p = 0$)	174	0.497	1.17
Elastomer ($m_p = 0$)	225	0.256	1.22
Spurr epoxy ($m_p = 0$)	266	0.519	1.75
Araldite ($m_p = 0$)	274	0.509	1.77
Porous araldite ($m_p = 0.10$)	323	0.456	1.92
Porous araldite ($m_p = 0.15$)	348	0.434	1.99
Porous araldite ($m_p = 0.20$)	373	0.414	2.06
Porous araldite ($m_p = 0.25$)	399	0.395	2.12
Porous araldite ($m_p = 0.30$)	426	0.376	2.18

^a From equation $d_h^*(m_{\text{opt}}, m_p) = \max d_h^*$.

^b m_p is the volume concentration of the spherical pores distributed regularly in the polymer matrix.

Table 5. Effective piezoelectric coefficients d_h^* (in pC N^{-1}), g_{33}^* , g_h^* (in mV m N^{-1}), squared figures of merit $(Q_{33}^*)^2$, $(Q_h^*)^2$ (in 10^{-12} Pa^{-1}) and electromechanical coupling factor k_{33}^* and k_t^* which have been calculated for the 1–0–3 PMN–0.33PT single crystal/porous araldite composite at $m_p = 0.30$.

ρ^a	$m_{\text{d,hyd}}^b$	d_h^*	g_{33}^*	g_h^*	$(Q_{33}^*)^2$	$(Q_h^*)^2$	k_{33}^*	k_t^*
10	0.252	998	149	74.1	300	73.9	0.941	0.920
100	0.120	1780	317	252	710	449	0.946	0.940
200	0.096	1920	399	335	910	644	0.946	0.942
300	0.083	1980	459	396	1050	783	0.946	0.942
400	0.077	2010	495	432	1140	869	0.947	0.943
500	0.073	2040	522	459	1210	934	0.947	0.943

^a The aspect ratio of the spheroidal pores in the polymer matrix.

^b The volume concentration $m_{\text{d,hyd}}$ of the single-crystal rods obeys condition $\max d_h^*(m, 0.3, \rho) = d_h^*(m_{\text{d,hyd}}, 0.3, \rho)$ at the fixed ρ value.

porous matrix provides the displacement of the maxima of $[Q_{33}^*(m, 0.3, \rho)]^2$ and $[Q_h^*(m, 0.3, \rho)]^2$ to the lower m values, e.g. for $(Q_{33}^*)^2$ from 0.088 at $\rho = 2$ to 0.060 at $\rho = 5$.

Second, the maximum of $d_h^*(m, 0.3, \rho)$ also shifts to the lower m values but this displacement becomes appreciable in the wide range of ρ . In our opinion, for piezotechnical applications one can propose the 1–0–3 composites that possess the maximum hydrostatic piezoelectric activity in addition to considerable piezoelectric sensitivity and electromechanical coupling. Taking the aspect ratio ρ from a wide range, we calculate a series of the effective parameters that are expected at $\max d_h^*(m, 0.3, \rho)$ (table 5). The increase in the ρ value results in increasing g_{33}^* , g_h^* , d_h^* , $(Q_{33}^*)^2$ and $(Q_h^*)^2$ at practically constant and very large k_{33}^* and k_t^* values. The effect of the aspect ratio on the above-given parameters is mainly associated with a change in the $c_{11,m}/c_{33,m}$ ratio of the elastic moduli of the porous matrix. Increasing ρ corresponds to softening of the polymer matrix in the OX_3 direction, and this softening enables the control of the piezoelectric response of the 1–0–3 composite at the fixed porosity m_p of the matrix. It should be added that the values of $\max d_h^*(m, 0.3, \rho)$ from table 5 are larger than those evaluated recently [24] for the 0–0–2–2 composites containing one or two relaxor-ferroelectric components (e.g. the PMN–0.33PT and PZN–0.045PT single crystals) and two monolithic polymer components. This advantage appearing at $5 < \rho < 10$ is associated with the important role of the porous matrix with the variable $c_{11,m}/c_{33,m}$ ratio.

In our study we have varied the porosity of the polymer matrix in the range $0 < m_p < 0.3$. With regard to

the typical mechanical properties of the polymer with 20–30 vol% porosity, it has been observed that the typical decrease in stiffness and strength of such materials is about one order of magnitude [25, 26], relative to the pore-free material. For a sensor material consisting of a porous polymer with a high stiffness piezo-active material (e.g. single-crystal rod in our 1–3-type composites), most of the applied mechanical load will be experienced by the piezoelectric phase. Therefore, the polymer strength is unlikely to be a significant problem. Similarly, for an actuator material consisting of a porous polymer and piezoelectric ceramic, the relatively small piezoelectric strain is unlikely to exceed the failure strain of the polymeric material.

3. Conclusions

In this paper we have predicted the effective electromechanical properties for 1–3 and 1–0–3 piezo-active composites based on single crystals of the relaxor-ferroelectric solid solutions. The basic variables used in the prediction are the chemical composition of the single-crystal component, volume concentrations of the single-crystal component and the pores in the polymer matrix as well as the aspect ratio of the spheroidal pores. Modelling and property predictions have been carried out within the framework of the model ‘rods + matrix’ proposed for the description of the composites with the monolithic (1–3 connectivity) or porous (1–0–3 connectivity) matrix with good agreement with the limited experimental data in the literature. Maximum values of the effective piezoelectric coefficients g_{33}^* , g_h^* , d_h^* and h_{33}^* , squared figures of merit

$(Q_{33}^*)^2$ and $(Q_h^*)^2$ and electromechanical coupling factor k_t^* have been determined for the 1–3-type composites based on the PMN– x PT or PZN– x PT single crystals with compositions close to the morphotropic phase boundary. The large values of the piezoelectric coefficients $g_{33}^* \sim 10^2 \text{ mV m N}^{-1}$, $g_h^* \sim 10^2 \text{ mV m N}^{-1}$ and $d_h^* \sim (10^2\text{--}10^3) \text{ pC N}^{-1}$ are attainable due to favourable relations between the electromechanical properties of the components and the presence of the system of the single-crystal rods with $d_{3j,c} \sim 10^3 \text{ pC N}^{-1}$. The correlation between the max d_h^* and $c_{11,m}/c_{12,m}$ values has been established for the 1–0–3 composites with spherical pores in the matrix and for the 1–3 composites with the monolithic matrix (see table 4). It has been shown that both high piezoelectric activity and considerable piezoelectric sensitivity are attained, particularly for the 1–0–3 PMN–0.33PT-based composite with a polymer matrix containing oblate spheroidal pores (see table 5). This information is of value for those considering the use of relaxor-ferroelectric single crystals as a component in 1–3 type piezoelectric composites.

Acknowledgments

The authors would like to thank Professor Dr A V Turik (Russia) and Dr M Kamlah (Germany) for their interest in the research problems.

References

- [1] Park S-E and Shrout T R 1997 *J. Appl. Phys.* **82** 1804
- [2] Noheda B 2002 *Curr. Opin. Solid State Mater. Sci.* **6** 27
- [3] Zhang R, Jiang B and Cao W 2001 *J. Appl. Phys.* **90** 3471
- [4] Ritter T, Geng X, Shung K K, Lopath P D, Park S-E and Shrout T 2000 *IEEE Trans. Ultrason. Ferroelectr. Freq. Control* **47** 792
- [5] Cheng K C, Chan H L W, Choy C L, Yin Q, Luo H and Yin Z 2003 *IEEE Trans. Ultrason. Ferroelectr. Freq. Control* **50** 1177
- [6] Lam K H, Chan H L W, Luo H S, Yin Q R, Yin Z W and Choy C L 2003 *Microelectron. Eng.* **66** 792
- [7] Ye Z-G and Dong M 2000 *J. Appl. Phys.* **87** 2312
- [8] Iwata M, Katsuraya K, Suzuki I, Maeda M, Yasuda N and Ishibashi Y 2003 *Japan. J. Appl. Phys. Pt.1* **42** 6201
- [9] Ye Z-G and Topolov V Yu 2001 *Ferroelectrics* **253** 79
- [10] Yin J and Cao W 2002 *J. Appl. Phys.* **92** 444
- [11] Zhang R, Jiang B, Cao W 2002 *J. Mater. Sci. Lett.* **21** 1877
- [12] Jiang W, Zhang R, Jiang B and Cao W 2003 *Ultrasonics* **41** 55
- [13] Cao H and Luo H 2002 *Ferroelectrics* **274** 309
- [14] Cao H, Schmidt V H, Zhang R, Cao W and Luo H 2004 *J. Appl. Phys.* **96** 549
- [15] Peng J, Luo H, He T, Xu H and Lin D 2005 *Mater. Lett.* **59** 640
- [16] Topolov V Yu and Kamlah M 2004 *J. Appl. Phys.* **37** 1576
- [17] Akcakaya E and Farnell G W 1998 *J. Appl. Phys.* **64** 4469
- [18] Glushanin S V and Topolov V Yu 2001 *J. Appl. D: Appl. Phys.* **34** 2518
- [19] Levassort F, Topolov V Yu and Lethieq M 2000 *J. Phys. D: Appl. Phys.* **33** 2064
- [20] Dunn M L and Taya M 1993 *J. Am. Ceram. Soc.* **76** 1697
- [21] Eshelby J D 1957 *Proc. R. Soc. Lond. A* **241** 376
- [22] Huang J H and Yu J S 1994 *Compos. Eng.* **4** 1169
- [23] Chan H L W and Unsworth J 1989 *IEEE Trans. Ultrason. Ferroelectr. Freq. Control* **36** 434
- [24] Grekov A A, Kramarov S O and Kuprienko A A 1989 *Mech. Compos. Mater.* **25** 54
- [25] Levassort F, Lethieq M, Certon D and Patat F 1997 *IEEE Trans. Ultrason. Ferroelectr. Freq. Control* **44** 445
- [26] Zheludev I S 1971 *Physics of Crystalline Dielectrics* (New York: Plenum)
- [27] Topolov V Yu and Turik A V 2001 *Tech. Phys.* **46** 1093
- [28] 2000 *ISIS News Edition* **31** 14 <http://www.isis-innovation.com/>
- [29] Topolov V Yu, Glushanin S V and Panich A E 2004 *Ferroelectrics* **308** 53
- [30] Ashby M F 2006 *Phil. Trans. R. Soc. A* **364** 15
- [31] Pal R 2005 *J. Compos. Mater.* **39** 1147